Articles in PresS. Am J Physiol Endocrinol Metab (April 3, 2012). doi:10.1152/ajpendo.00594.2011

Normal Human Melanocytes Exposed to Chronic Insulin and Glucose Supplementation Undergo Oncogenic Changes and Methyl Group Metabolism Cellular Redistribution

DANIEL MORVAN[1], JEAN MARC STEYAERT[2], LAURENT SCHWARTZ[3], MAURICE ISRAEL[4], and AICHA DEMIDEM[1].

Author contributions: Daniel Morvan and Aicha Demidem contributed equally to this study.

Affiliations:

[1]INRA UMR1019, Centre de Clermont-Ferrand, Theix, 63122 Saint-Genès Champanelle France.

[2]Ecole Polytechnique, Laboratoire d'informatique, 91128, Palaiseau, France.

[3]Hopital Poincaré, 104 Bvd Poincaré, 92 380 Garches, France.

[4] Societé Biorebus, Paris, France.

Running head: Melanocyte Response to Insulin and Glucose Supplementation

Correspondance to: Dr Aicha Demidem, UNH 1019, Centre INRA de Clermont-Ferrand, 63122 Saint Genes Champanelle, France.

Email : ademidem@clermont.inra.fr

ABSTRACT

Recent epidemiologic studies have suggested a link between cancer and pathophysiological conditions associated to hyperinsulinemia. In this report, we addressed the possible role of insulin exposure in melanocyte transformation. To this aim, normal melanocytes were exposed to chronic insulin and glucose supplementation (×2 the standard medium concentration) for at least 3 weeks. After 3 weeks treatment, melanocytes increased proliferation (doubling time: 2.7 vs 5.6 days, $P<0.01$). After 3 weeks treatment or after 3 weeks treatment followed by 4 weeks re-culture in standard medium, melanocytes were able to grow in soft agar colonies. Treated melanocytes had increased DNA content (+8%, $P<0.05$), chromosomal aberrations, and modified oncoprotein profile: PAkt expression increased (+32%, $P<0.01$), Akt decreased, and c-Myc increased (+40%, $P<0.05$). PP2A protein expression increased (+42, $P<0.05$) while PP2A methylation decreased (-42%, $P<0.05$), and PP2A activity was reduced (-27%, $P<0.05$). PP2A transcription level was increased (*ppp2r1a*, PP2A subunit A, +44%, $P<0.05$). Also, transcriptomic data revealed modifications in *insr* (insulin receptors, +10%, $P<0.05$) and *Il8* (inflammation protein, +99%, $P<0.01$). Glycolysis was modified with increased transcription of *Pgk1* and *Hif1a* ($p<0.05$), decreased transcription of *Pfkfb3* ($P<0.05$), decreased activity of pyruvate kinase ($P<0.01$), and decreased pyruvate cell content as assessed by ^{1}H-NMR spectroscopy. In addition, methyl group metabolism was altered with decreased global DNA methylation (-51%, $P<0.01$), increased cytosolic protein methylation (+18%, $P<0.05$), and consistent changes in methylated species on ^{1}H-NMR spectra. In conclusion, exposure to chronic insulin and glucose supplementation induces oncogenic changes, and methyl group metabolism redistribution which may be a biomarker of transformation.

Keywords

Melanocytes; chronic insulin and glucose supplementation; oncoproteins; PP2A; methyl group metabolism.

INTRODUCTION

Cancer is a multistep process, in which genetic alterations have a cumulative effect on the control of cell proliferation, division and growth control. Genetic instability has been prominently implicated in tumor formation. The main evidence comes from the discovery of chromosomal aberrations and mutations of oncogenes or tumor suppressor genes (25). There is experimental evidence that gene alterations can result from viral infection or carcinogenic insult (25).

In vivo, among normal epidermis cells, Langerhans cells and melanocytes are not able to proliferate to the contrary of keratinocytes. In vitro, melanocytes can be cultured under highly specific conditions (11). Transformation capabilities of melanocytes are well known in relation to exposure to UV (9). However, a recent study raised doubt about the exclusive role of UV in melanocytes carcinogenesis (26). In vitro studies on human melanocytes and skin, and mouse models continue to refine knowledge on the specific effects of UV on normal and genetically susceptible melanocytes. Epidemiologic data on the effects of UV on melanocyte transformation remain controversial (26) (38).

Recent studies have suggested a link between certain cancer types and pathophysiological conditions associated to hyperinsulinemia, including type 2 diabetes, metabolic syndrome, obesity, as well as chronic inflammation, all conditions which incidence is rising in western countries (22). Recent in vivo studies in mice have demonstrated the effect leptin, a product of obese (*ob*) gene, secreted by adipocytes, as a promoter of tumor growth (3). Chronic hyperinsulinemia was shown to favour melanoma tumor growth by inhibiting apoptosis and stimulating cell proliferation in the so-called insulin-cancer (14). In addition, it has been reported that insulin resistance may be an independent risk factor for melanoma (4).

In this article, we sought whether exposure to chronic insulin and glucose supplementation could promote melanocyte transformation. To evaluate carcinogenesis, classical criteria were investigated including cell proliferation rate, soft agar colony formation, DNA content, karyotype, oncoprotein expression (PP2A, Akt/PAkt, cMyc, PTEN, PP1 and Ras), PP2A activity which has been shown to be decreased in tumor cells (19). Metabolic alterations were explored including glycolysis and methyl group metabolism.

We found that normal human melanocytes (NHM) exposed to chronic insulin and glucose supplementation display increased proliferation and form colony on soft agar. Also, these cells exhibit increased DNA content, alteration of karyotype, oncoprotein profile changes including increased expression of PP2A, P-Akt and cMyc. In contrast, PP2A methylation and activity were decreased. Transcriptomic data revealed consistent changes in PP2A regulation, *Il8* inflammation mediator, and glycolysis. In addition, treated cells exhibited methyl group metabolism redistribution between nucleus and cytoplasm.

In conclusion, our data establish that chronic exposure to chronic insulin and glucose supplementation induces oncogenic changes and methyl group metabolism redistribution which raises the hypothesis of a relationship between cellular oncogenic signalling and methylations. These findings are, to our knowledge, the first demonstration of the potential of chronic insulin and glucose supplementation to promote a pre-cancerous state in human melanocytes.

MATERIALS AND METHODS

Chemicals

Glucose and insulin were purchased from Sigma. Glucose was used after dissolution in distillated water. Okadaic acid (Sigma, Saint Quentin Fallavier, France) was prepared as a 50 nM stock in DMSO. All these reagents were used in vitro in cell cultures. L-[$^{14}CH_3$]-S-adenosyl methionine (L-[$^{14}CH_3$]-SAM) (55 mCi.mmol^{-1} specific activity) was purchased from Amersham Bioscience (Buckinghamshire, UK). TRIzol® reagent was purchased from Gibco.

Cell Culture and Cell Treatments

Normal human melanocytes (NHM) were obtained from foreskin of kids aged 5-7 years. After trypsinisation, cells were cultured and maintained in a specific medium (Tebu); this medium contain insulin at 5 µg/ml and glucose at 1.081g/ml. Others cells lines were used, as including murine B16 melanoma, murine fibroblasts L929 and human tumor ocular melanoma IPC 227F. These cells lines were maintained as monolayer in culture flasks in Eagle's MEM-glutaMAX medium (Gibco) supplemented with 10% fetal calf serum (Sigma), 1 mM sodium pyruvate, 4 µg/ml gentamicin, 200 mM glutamine, 1x non-essential amino-acid solution (Gibco) and vitamin (Gibco). To determine growth curves, cells were cultured in triplicate wells in 12-well plates and counted every 2 days.

The dose-proliferation relationship of insulin and glucose supplementation was performed at various concentrations including 1-, 2-, 5-,7-, 10- and 50-fold the concentration of the standard medium (insulin, 5 µg/ml and glucose, 6 mM). For the rest of the study the insulin and glucose supplementation was ×2 the insulin-glucose concentration of the standard medium. Cell culture was followed for 3 to 7 weeks. Treated human melanocytes were

separated in two groups, one exposed to ×2 insulin-glucose supplementation with the medium changed twice a week and followed over more than 3 weeks (ING), and the other treated for 3 weeks then recultured into standard medium without treatment for 4 weeks (ING*).

Cell cycle analysis

Melanocyte pellets were snap-frozen in liquid nitrogen during 10 min before use. The cells were incubated with R5125 RNAse A (Sigma-Aldrich, St-Quentin Fallavier, France) and 50 µg/µl propidium iodide (Sigma-Aldrich) for 15 min at +4°C in the dark. The stained cells were run in an EPICS XL flow cytometer (Beckman Coulter, Roissy CDG, France), and data was analyzed with MultiCycle software (Phoenix Flow Systems, San Diego, CA).

Colony Formation in Soft Agar

Colony-forming efficiency was determined using a double-layer soft-agar method. Cells (2×10^3 per dish) were suspended in 1.5 ml of 0.3% Noble agar supplemented with complete culture medium containing ×2 insulin and glucose. This suspension was layered over 1.5 ml of a 0.6% agar medium base layer containing ×2 insulin and glucose in 35 mm culture dishes (Nuclon). After 20 days, cells colonies were counted.

Karyotype

Untreated and insulin-glucose treated human normal melanocytes were cultured as monolayer in culture flasks until 70% confluence, and then treated with colchicine at (0.01 µg/ml) for 17 to 57 h.

Radiolabeling Study of Cellular Methylations

For investigation of cellular methylations, melanocytes were incubated with 0.8 µCi/ml of L-[$^{14}CH_3$]-S-adenosylmethionine (SAM) during 5 days before collection in order to achieve steady state level of radioactivity into the cells. Cells were divided in 2 groups, one was left untreated, and the other one was treated by insulin and glucose. At different times cells were harvested for analysis.

Total Cell Protein Extracts and Protein Concentration

Intact cells in a lysis buffer (50 mM Tris HCl pH 8, 100 mM NaCl) containing protease inhibitor mixture (Roche, Mannheim, Germany) were lysed by ultrasonication (3 times 15 s in ice). After centrifugation (14,000 *g*, 10 min at 4°C), the supernatant was kept at -80°C until analysis. Protein concentration was determined with Commassie Blue (Pierce) at lambda 595 nm with bovine albumin serum as a standard.

Cell Fractionation

All the extraction procedure was done in ice. Cells were Dounce homogenized with pestle "B" in fractionation buffer (10 mM Tris HCl pH 7.4, 10 mM NaCl, 3 mM $MgCl_2$, 1 mM EDTA) containing protease inhibitor mixture. Complete cells lysis was checked by microscopy with Trypan Blue. Then lysed cells were centrifugated (10,000 *g*, for 10 min at 4°C). Supernatant was kept as the cytosolic fraction. The pellet was carefully washed with lysis buffer and centrifugated (10,000 *g*, for 10 min at 4°C). The supernatant was added to the cytosolic fraction. The pellet containing nuclei was further disrupted by ultrasonication

in fractionation buffer (3 times 15 s in ice) and centrifugated (10,000 *g*, for 10 min at 4°C). The supernatant was kept as the nuclear fraction.

Radiolabel Incorporation in Proteins

For the study of methyl group incorporation in cytoplasmic and nuclear proteins, cells were Dounce homogenized with pestle "B" in a fractionation buffer (10 mM Tris HCl pH 7.4, 10 mM NaCl, 3 mM $MgCl_2$, 1 mM EDTA) containing protease inhibitor mixture. Complete cell lysis was checked by microscopy with Trypan Blue. Then lysed cells were centrifuged (10,000 *g* for 10 min at 4°C). Supernatant was kept as the cytosolic fraction. The pellet was carefully washed with lysis buffer and centrifuged (10,000 *g* for 10 min at 4°C). The supernatant was added to the cytosolic fraction. The pellet containing nuclei was further disrupted by ultrasonication in fractionation buffer (3 times 15 s in ice) and centrifuged (10,000 *g* for 10 min at 4°C). The supernatant was kept as the nuclear fraction. Proteins from the cytoplasmic and the nuclear compartments were precipitated by adding 4 volumes of cold acetone to the cytoplasmic and nuclear fractions. The homogenates were vortexed, stored at -20°C for 2 h and then centrifuged (14,000 *g*, 30 min at 4°C). The pellet containing the precipitated proteins was washed twice in acetone. Then acetone was evaporated under nitrogen stream. The pellets were mixed with 1 M NaOH and protein concentration was determined. An aliquot of the protein solution was mixed with liquid scintillation cocktail (Packard, Rungis, France), the radioactivity was measured in a scintillation counter (Winspectral Wallac 1414). Radioactivity incorporation was expressed as the percentage of dpm in insulin and glucose-treated cells proteins compared to untreated cell dpm values. Three independent experiments were performed.

Radiolabel Incorporation in DNA

DNA was extracted by the TRIzol® method according to the manufacturer's instructions and its concentration was determined at lambda 260 nm. Then, 5 µg of the dissolved DNA was mixed with 4.5 ml of a liquid scintillation cocktail (Ultima Gold, Packard), and the radioactivity was measured in a scintillation counter. Radioactivity incorporation was expressed as dpm/µg DNA. Data represent three independent experiments.

Western Blot

Twenty micrograms of proteins from total cells and from the cytoplasmic and nuclear fractions were subjected to SDS-PAGE on 10% SDS-polyacrylamide gels and transferred onto Immobilon-NC membrane (Millipore). The membrane was blocked in 4% nonfat milk/TBST (25 mM Tris HCl pH 8, 125 mM NaCl, 0.1% Tween 20) at 4°C overnight, and probed with antibodies against PP2Ac subunit (1:2,500), methylated PP2Ac subunit (1:250), PP1 (1:2,000) (Upstate, Lake Placid, NY), Akt (1:1,000), phosphorylated Akt or PAkt (Ser^{473}) (1:1,000), phosphorylated PTEN (Ser^{380}/$Thr^{382/383}$) (1:1,000), PTEN (1:1,000) (Cell Signaling), c-Myc (1:200) (Santa Cruz Biotechnology), Ras (1: 2,000) and β-tubulin (1:2,500) (Sigma) overnight at 4°C and washed three times with TBST. Bound antibodies were detected with horseradish peroxydase-conjugated secondary antibody IgG (Upstate, Lake Placid, NY) using enhanced chemiluminescence Western blotting detection reagents (Amersham Bioscience, Buckinghamshire, UK). Equal loading of proteins was checked by Ponceau S staining of the membranes. Densitometrical measurement of the band of interest was done using the Quantity One software (BioRad). Normalization was done using β-tubulin densitometrical values. Data are representative of three independent experiments.

As a control for PP2A methylation on Western blots, okadaic acid (OA), an antagonist of PP2A methylation, was added to the culture medium of untreated NHM, at 5 nM for 48 h. Following treatment by OA, cells were rinsed in PBS and maintained in fresh culture medium for few days (5 to 7 days). Then Western blots were performed to evaluate PP2A expression. The time exposure of OA was based on reference (19).

Metabolic Profiling by ^{1}H-NMR spectroscopy

Proton NMR spectroscopy of intact cells was performed at 500 MHz using a high resolution magic angle spinning coil (Bruker). The NMR sequence was a saturation recovery sequence with acquisition and processing parameters reported in reference (25). ^{1}H-NMR spectra were line-broadened and phased. Signal attributions have been reported in references (29) (6).

PP2A Phosphatase Activity

A PP2A immunoprecipitation phosphatase assay kit (Upstate) was used to detect PP2A activity according to the manufacturer's instructions. PP2A was immunoprecipitated with a monoclonal anti-PP2A antibody and protein A-Sepharose beads in lysis buffer. PP2A-bound beads were washed with phosphatase assay buffer and then with pNPP serine/threonine assay buffer (50 mM Tris HCl, 100 mM $CaCl_2$, pH 7.0; Upstate). Diluted phosphopeptide (K-R-pT-I-R-R) in serine/threonine assay buffer (250 µM) was added and then incubated for 15 min at 30°C. After centrifugation, 25 µl of supernatant was transferred to an assay plate, and 100 µl of Malachite Green phosphate detection solution was added for 15 min incubation at 30°C. The relative absorbance was measured at 630 nm wavelength. Data are representative of two independent experiments that were performed in duplicate.

Pyruvate Kinase Activity

An aliquot of total cell protein extracts was incubated in 50 mmol/L Tris-HCl pH 7.4, 100 mmol/l KCl, 5 mmol/l $MgCl_2$, 0.6 mmol/L ADP, 0.9 mmol/l phosphoenolpyruvate, 0.3 mmol/L NADH and 2.5 IU L-lactate dehydrogenase. Pyruvate kinase activity was measured at 25°C for 5 min by recording NADH oxidation at 340 nm and was calculated using A_{340}/min obtained from the initial linear portion of the curve, with one unit of activity defined as that required for the oxidation of 1 μmol NADH min^{-1} mg^{-1} protein at 25°C and pH 7.4.

Transcriptomics

In order to study mechanisms of melanocyte transformation, we used the TaqMan Low Density Array technique (Applied Biosystems) to screen 89 genes associated with cell cycle and signalling, oncoproteins and PP2A, bioenergetic metabolism, lipid metabolism, methyl group metabolism and other metabolic pathways and oxidative stress.

Statistical Analysis

In all experiments, data are given as mean ± SD. Comparison between groups was performed using the Student's t-test.

RESULTS

Chronic Insulin and Glucose Supplementation Promotes Melanocyte Proliferation

Exposure of normal human melanocytes to chronic insulin and glucose supplementation (ING and ING* cells) increased cell proliferation (Fig. 1*A*). ING cells exposed to concentrations of ×2 to ×10 exhibited shortened doubling time (Table 1). At ×2 insulin-glucose supplementation, the doubling time was 2.7 *vs* 5.6 days ($P<0.01$); at ×5 to ×10, the doubling time was collectively 3.4 days. In contrast, at ×50, cell proliferation strongly decreased (doubling time = 15 days) showing that treatment has become overtly toxic.

As shown in Fig. 1*A*, the proliferation curve of ING* cells (treated for 3 weeks with ×2 insulin-glucose supplementation, then recultured for 4 weeks without treatment) was superposed to that of ING cells.

ING* cells had modified morphology, with a large cytoplasm, and a long extension of cytoplamic membrane, without any signs of blebbing or indentations of the nuclear membranes (Fig. 1*B*). ING* cells displayed decreased proportion in the G1 phase of the cell cycle and increased proportion in phase G2 (22 % *vs* 14%, ING* vs UN) and in phase S (25 % *vs.* 11%, ING* vs UN) (Fig. 1*C*).

Chronic Insulin and Glucose Supplementation Induces Colonies in Soft Agar

The ability of insulin-glucose-treated melanocytes to form colonies in soft agar is a classical marker for cell transformation (i.e., these cells display anchorage-independent growth). Several types of cells were tested: untreated human melanocytes (UN), insulin and glucose-treated human melanocytes (ING) and (ING*), B16 murine melanoma cells and L929 transformed fibroblasts. Among these cell types, only untreated melanocytes were unable to

form colonies in soft agar (Fig. 2*A*). Quantification of the number of colonies of the different cell lines is shown in Fig. 2*B*.

Chronic Insulin and Glucose Supplementation Provokes DNA and Chromosomal Alterations

Insulin and glucose exposure increased DNA content of treated cells (+8% $P<0.05$) as shown in Fig. 3*A*. The karyotype of untreated and insulin-glucose treated melanocytes was performed. ING* cells exhibited an increase in the amount of chromosomes (46 vs 94, ING* vs UN) even if the number of concerned chromosomes could not be specified. In addition, chromosome arms were extended, suggesting activated telomerases (arrows, Fig. 3*B*).

Chronic Insulin and Glucose Supplementation Induces Changes in Oncoprotein and PP2A Expression

In treated cells, Akt expression was decreased, P-Akt expression increased (+32% and +35%, $P<0.05$, ING and ING* vs UN, respectively), c-Myc expression increased (+36% and +54%, $P<0.05$, ING and ING* vs UN, respectively) and Ras expression increased (Fig. 4*A*). PP1 expression varied poorly (Fig. 4*A* and *B*). PTEN and P-PTEN, an oncosuppressor activated by phosphorylation, varied poorly (Fig. 4*A*). The ocular melanoma cell line IPC displayed a similar oncoprotein profile than ING and ING* cells (Fig. 4*B*), in favor that ING and ING* cells underwent oncogenic changes. Because ING* cells maintained the oncogenic profile despite they were recultured in standard medium for 4 weeks, it may be concluded that the transformed phenotype was acquired during the first 3 weeks of treatment.

As shown in Fig. 4*A* and *B*, normal melanocytes expressed high levels of PP2AC subunits, both methylated C and non methylated. During exposure to chronic insulin and glucose supplementation, PP2AC expression was increased (+60% and +47%, $P<0.05$, ING and

306 ING* vs UN, respectively), the methylated C subunit of PP2A was decreased (-42%
307 P<0.05).
308 As a control for PP2A methylation and its consequences on oncoprotein regulation, normal
309 human melanocytes were treated by OA, an antagonist of PP2A. OA inhibited methylation
310 of PP2A (-50%) which up-regulated P-Akt (+30%) and c-Myc (+35%) (Fig. 4*C*), showing
311 that inhibiting the activity of PP2A promoted oncogenic changes in melanocytes.
312 The activity of PP2A phosphatase activity was assayed and found to be decreased (-27% and
313 -30%, P<0.05, ING and ING* vs UN, respectively), in agreement with decreased
314 methylation of PP2A. As a matter of comparison, PP2A activity was markedly diminished in
315 ocular melanoma IPC tumor cells (-42%, IPC vs UN, P<0.01) (Fig. 4*D*).
316
317 The regulation of oncoproteins and PP2A was investigated by transcriptomics (Table 2). Only
318 some oncoproteins and oncosuppressors had altered transcription. In ING* cells, *Nras* was
319 downregulated (-38%, p=0.044) and *Pink1*, upregulated (+71%, p=0.038). *Myc* and *Kras*
320 decreased although their variations were less significant (P<0.10). *Akt1* did not vary
321 significantly. Data showed upregulation of *ppp2r1a* (subunit A of PP2A, +44%, P<0.05),
322 downregulation of *Ppp1ca* (P<0.05) but the lack of variation of *Pppc1b*, and upregulation *of*
323 *lcmt1* (leucine carboxy_methyl transferase, +26%, P<0.05).
324 As could be expected, insulin-glucose treatment upregulated *Insr*, insulin receptor, (+10%,
325 p=0.017) and *Ccnd1* (+52%, p=0.037), in relation with increased proliferation. Interestingly,
326 *Il8*, a marker of inflammation, was markedly upregulated (+99%, p=0.007). Inflammation is
327 a condition that favours carcinogenesis.
328
329 *Chronic Insulin and Glucose Supplementation alters Glycolysis*

In ING* cells, bioenergetics-associated transcriptomic data showed the following alterations (Fig. 5*A*): *Slc2a3* (+26%, p=0.075), *Pfkfb3*, which encodes for 6-phosphofructo-2-kinase/fructose-2, 6-biphosphate 3, (-49%, p=0.033), *pgk1,* which encodes for phosphoglycerate kinase, (+33%, P=0.007), *Hif1a* (+59%, p=0.041). In addition, *Pdk1* and *Pkm2* moderately increased, although their variations were less significant (P<0.10). Pyruvate kinase activity was markedly reduced in ING and ING* cells (-42% and -39%, P<0.01, ING and ING* vs UN, respectively), which compared to that of ocular melanoma IPC 227F tumor cells (-48%, IPC vs UN) (Fig. 5*B*). As shown by ^{1}H-NMR spectra, pyruvate (Pyr, signal at 2.37 ppm) and oxaloacetate (OAA, signal at 2.38 ppm), an intermediate of the Krebs cycle, were decreased in ING* cells in comparison with NHM. In addition, alanine (Ala, signal at 1.47 ppm) and glutamate (Glu, signal at 2.35 ppm) levels were increased in IPC melanoma tumor cells, in comparison with ING* cells. Ala and Glu are derivatives of the transamination of Pyr and OAA (Fig. 6*A*). Taken together, these data are in favour that the phenotype of transformed human melanocytes has become more glycolytic, similarly to tumor cells.

Insulin and Glucose Supplementation induce Cellular redistribution of methyl group metabolism

In ING* cells, methyl group metabolism-related transcriptomic data showed the following alterations (Table 2): *Lcmt1,* which encodes for PP2A methyltransferase, (+26%, P<0.05), *Pemt,* which encodes for phosphatidylethanolamine methyltransferase, (+31%, P<0.05) and *Mgmt,* which encodes for O(6)-alkylguanine methyltransferase (+32%, P<0.05).

The distribution of methyl group metabolism was investigated in cellular and molecular compartments of insulin-glucose treated cells. Incorporation of radioactivity from L-[$^{14}CH_3$]-

SAM was decreased in nucleic proteins (-51%, ING* vs UN, P<0.01), and increased in cytoplasmic proteins (+18%, ING* vs UN, P<0.05) (Fig. 6*B*). DNA methylation was decreased (-8%, ING and ING* vs UN, P<0.05) (Fig. 6*C*).

Methyl group metabolism alteration were visible in ^{1}H-NMR spectra of ING* cells, in comparison to UN and IPC cells (Fig. 6*A*). ^{1}H-NMR spectra, which mostly reflect cytoplasmic content, showed, in ING* cells, in comparison with NHM: decreased levels of methyl acceptors: glycine (Gly) (signal at 3.56 ppm) and guanidino-acetate (GA) (signal at 3.75 ppm), and increased levels of sarcosine (Sar) (methyl signal at 2.73 ppm), which is both the methylated form of Gly and a methyl donor. In IPC tumor cells, in comparison with ING*, ^{1}H-NMR spectra showed: increased levels of creatine (Cr) (methyl signal at 3.03 ppm), the methylated form of GA, and decreased levels of glycerophosphocholine (GPC) (methyl signal at 3.23 ppm), a methyl donor.

Taken together, these data show that chronic insulin and glucose supplementation shifts cellular methyl group metabolism from the nucleus to the cytoplasm.

Other metabolic changes induced by chronic insulin and glucose supplementation

Transcriptional data showed changes in lipid and phospholipid metabolism (Table 2), including *Acly* (-33%, p=0.023), *Fasn* (-70%, P<0.05), *Pcyt1b* (+%140.46, P<0.05), *Chpt1* (+31%, p=0.032), P*la2r1* (+103%, P<0.05), and *Plcb4* (+24%, p=0.042). Proton-NMR spectra showed a decrease in glycerophosphocholine (a product of phosphatidylcholine hydrolysis) in IPC tumor cells in comparison with ING* cells. Some of these data may appear controversial or indicate that, in ING* cells, lipid metabolism has not passed the oncogenic transition, yet.

Also transcriptomics showed alteration in oxidative stress pathways in insulin-glucose treated cells, including *Txnrd1* (+72%, p=0.034), *Gss* (+19%, p=0.045) and *Gsr* (-9%, p=0.007). In agreement with these data, ^{1}H-NMR spectra showed an increased content in GSH in IPC melanoma tumor cells in comparison with ING* cells. These data are in favour that oxidative stress took place early in the process of transformation.

DISCUSSION

This study establishes that normal human melanocytes exposed to chronic insulin and glucose supplementation undergo oncogenic changes including proliferation, ability to grow in colonies, chromosomal abnormalities, increased oncoprotein expression and decreased PP2A activity. These disorders are associated to metabolic alterations of oncogenic type including increased glycolysis and oxidative stress response, and to cellular redistribution of methyl group metabolism.

In vivo, exposure to chemical carcinogens or radiation is considered as a major factor of normal cell transformation or carcinogenesis in human cancers (25). However, *in vitro*, carcinogens alone have not successfully transformed normal human cells in culture (15) (27) (35). To undergo transformation, normal cells need prior to exposure to a carcinogen to be immortalized by transfection with a cancer-associated virus (10).

During carcinogenesis, tumor promotion is usually preceded by an intense inflammatory reaction, itself resulting from the action of a tumor initiator. The effect of genotoxic carcinogenic compounds is not limited to epithelial cells. It causes extensive tissue damage resulting in the release of free radicals and chemicals through cell killing and replacement.

Forty per cent of chemicals that are carcinogenic in chronic animal tests are not mutagenic (8). These non genotoxic compounds do not cause DNA damage.

As a genotoxic agent, ionizing radiations induce cancers in humans and in animals (16) (12). However, like for chemical carcinogenesis, numerous attempts to achieve transformation of normal human cells *in vitro* have been generally unsuccessful (34).

Genetic instability has been implicated in tumor formation. It is possible that the stress secondary to massive glucose influx increases the mutation rate (1). Non genotoxic stress such as heat or serum starvation can induce a mutator phenotype with persistent and pronounced genetic instability. Perhaps triggered by exposure to carcinogens or abnormal physiological conditions, this hypermutable state could cause mutations in many genomic loci in a normal cell (25).

In this paper, we used normal human melanocytes and demonstrated that chronic insulin and glucose supplementation (×2 the standard medium concentration) without any other carcinogen can induce a mutator phenotype with up-regulation of several oncoproteins.

The combination of insulin and glucose was used to prevent a possible nutritional cause for impeding proliferation over the long term, and because the phenotype of human melanocytes was expected to become more glycolytic, which was confirmed by transcriptional analysis. Glucose at ×2 (about 12 mM) did not cause an osmotic shock because of rapid transport of glucose, further favored by administration of insulin, and metabolism of glucose (glycolysis). Increased transport of glucose was testified in insulin-glucose supplemented melanocytes by transcriptional data.

The relationship between insulin and glucose uptake and oncogene activation is a complex one (18). In, this study, without genetic manipulation, we found that insulin-glucose treated normal melanocytes develop several criteria of transformation, commonly found in melanoma tumor cells, including increased rate proliferation, formation of colonies in soft agar, karyotype and DNA alterations, increased oncoprotein expression, decreased PP2A activity, and metabolic alterations commonly reported in tumors, increased glycolysis and oxidative stress response.

Several studies have reported that oncogene transfection or virus introduction such SV40, result in malignant transformation of normal cells (10). In this study, chronic insulin and glucose supplementation induces an up-regulation of oncoproteins, (P-ATK and c-Myc and Ras) which sign the pre-cancerous state of treated melanocytes.

PP2A regulates cell proliferation through the activation of oncoproteins including Akt and c-Myc (5) (19) (32). The Akt/PKB pathway is involved in cell proliferation, protein synthesis, resistance to apoptosis (7) (2) (34). This pathway is often hyperactivated in cancer (37). It has been shown that glucose metabolites (citrate and phosphoenolpyruvate) inhibit PP2A carboxymethylation (31). In this study, glycolysis was upregulated, which may provide a link with decreased methylation and activity of PP2A.

At the molecular level, PP2A activity is regulated by the carboxymethylation of its catalytic subunit (24) (23). According to Fig. 7, insulin-glucose supplementation may provoke inhibition of LCMT1, activation of PME-1, and/or rerouting of S-adenosylmethionine (SAM) metabolism. Given the fact that *ppme1* transcript, encoding for PME-1, did not vary, *Lcmt1* was positively regulated, it is possible that SAM rerouting accounted for PP2A demethylation. Indeed insulin-glucose treated cells may be the place for intense competition

for the substrate SAM, required by most transmethylations. *Lcmt1* may be increased as a means for PP2A to dampen its demethylation.

Among genes differentially regulated in cells treated by insulin and glucose, *Il8*, Interleukin-8, was increased by 2 fold. *Il8* upregulation may indicate chronic inflammation, a condition favouring carcinogenesis. This may allow initiation and/or promotion during early carcinogenesis. Interleukin-8 (IL8/CXCL8) has been described as a key effector in cancer progression and metastases (20). It has been underlined that, *in vitro*, the phenotype of melanoma cells is defined by features of high proliferation and non invasiveness in contrast to weak proliferation and high invasiveness (17). These phenotypes are correlated to increased gene expression of Microphthlalmia-associated transcription factor (Mitf) (17). Mitf is critical for the regulation of melanocyte development and survival, and is closely related to the proliferative phenotype whereas the Wingless-type MMTV integration site family 5A (Wnt5A) expression is mostly related to invasiveness capability.
In our study, insulin-glucose treated melanocytes have switched on *Mitf* under the effect of microenvironment loaded in insulin and glucose. The increased expression of *Mitf* suggests that these cells acquired a proliferative phenotype rather than an invasive one, despite we did not evaluated Wnt5A expression level. In addition, *Mitf*-positive melanocytes (ING cells) have a high expression of *Cdkn2a*, which is implicated in cell proliferation. (21).

Glycolysis was upregulated in cells exposed to insulin-glucose as testified by transcriptional, enzymatic and metabolic changes in this study. *pgk1* and *hif1ą* increased expression and PK activity inhibition have been reported as markers of the so called “aerobic glycolysis”, a major biochemical trait of tumor cells (13) (1). Also glucose transporters were moderately

upregulated (*Slc2a1*, *Slc2a3*). The latter change, which accompanies aerobic glycolysis, accounts for strong glucose uptake of melanoma (and other) tumors on FDG scans (33).

Methyl group metabolism alterations have been associated to cancer. Global DNA hypomethylation but hypermethylation of specific tumor suppressor genes is a hallmark of cancer. A number of epidemiological and clinical studies have shown a link between methyl group or folate deficiency and tumorogenesis. Ina addition, DNA methylating agents have proved efficient in the treatment of some tumor types including melanoma. However the exact mechanism by which hypomethylation promotes neoplastic transformation remains unelucidated. Consistently with these data, chronic exposure to insulin and glucose supplementation induced a global demethylation of DNA. In addition, the transcription of *Mgmt*, which encodes for an enzyme demethylating DNA, was upregulated.

Besides genomic methylation abnormalities, tumor cells have been shown to have cytoplasmic methyl group metabolism alterations including a high content in methylated acceptors, creatine and phosphatidylcholine, and other methylated acceptors found in proteins like asymmetric dimethylarginine and trimethyllysine (29). In insulin-glucose-treated vs untreated melanocytes, metabolic profiling based on ^{1}H-NMR spectra, which mostly reflect cytoplasmic changes, showed decreased levels of methyl acceptors (GA, Gly) and Sar transient increase. Sar is a methylated form of Gly and was shown to increase in prostate tumor tissue due to increased activity of glycine-N-methyltransferase (GNMT) in relation with invasiveness (36).

GNMT is a major regulator of methyl group metabolism, also involved in diabetes that has been shown to be associated to liver methyl group metabolism abnormalities, including increased activity of glycine-N-methyltransferase (30). In addition, in insulin-glucose treated

melanocytes, *Pemt,* which encodes for a cytoplasmic enzyme methylating phosphadylethanolamine into phosphatidylcholine, was upregulated, and PP2A was demethylated. It has been reported that methylation of PP2A catalytic subunit was the most important methyl group consumer among the cellular proteins (19) (23). Thus not only GNMT but PP2A may be important actors of methyl group metabolism redistribution.

Taken together, our findings raise the question as to whether global DNA demethylation and methyl group metabolism redistribution within the cell could result from a competition between methyltransferases for the substrate SAM. In addition, methyl group metabolism redistribution could be an early event in the process of transformation besides upregulated glycolysis and oxidative stress response pathways.

In conclusion, human normal melanocytes exposed to chronic insulin and glucose supplementation undergo oncogenic changes and cellular redistribution methyl group metabolism. This model may serve understanding the relationship between cellular oncogenic signalling and methylations. These findings are, to our knowledge, the first demonstration of the potential of chronic insulin and glucose supplementation to promote cell transformation.

ACKNOWLEDGEMENTS

The authors thank Mathilde Bonnet Duquennoy for her technical assistance (transcriptomic analysis) and Samuel Guenin for his technical assistance (cell cultures).

GRANTS: Institut National de la Santé et de la Recherche Médicale (INSERM), and Biorebus Society.

DISCLOSURES: No conflicts of interest, financial or otherwise, are declared by the authors.

REFERENCES

1. **Ahmed N and Berridge MV.** Transforming oncogenes regulate glucose transport by increasing transporter affinity for glucose: contrasting effects of oncogenes and heat stress in a murine marrow-derived cell line. *Life Sci* 63: 1887-1903, 1998.

2. **Altomare DA and Testa JR.** Perturbations of the AKT signaling pathway in human cancer. *Oncogene* 24: 7455-7464, 2005.

3. **Amjadi F, Javanmard S**, **Zarkesh-Esfahani H**, **Khazaei M** and **Narimani M.** Leptin promotes melanoma tumor growth in mice related to increasing circulating endothelial progenitor cells numbers and plasma NO production. Exp Clinical cancer Res, 30: 21-27, 2011.

4. **Antoniadis A, Petridou E, Antonopoulos C, Dessypris N and Panagopoulou P**. Insulin resistance in relation to melanoma risk. Melanoma Res, 21: 541- 546, 2011.

5. **Arroyo JA, Konno T, Khalili DC, and Soares MJ.** A simple in vivo approach to investigate invasive trophoblast cells. *Int J Dev Biol* 49: 977-980, 2005.

6. **Bayet-Robert M, Loiseau D, Rio P, Demidem A, Barthomeuf C, Stepien G, and Morvan D.** Quantitative two-dimensional HRMAS 1H-NMR spectroscopy-based metabolite profiling of human cancer cell lines and response to chemotherapy. *Magn Reson Med* 63: 1172-1183, 2010.

7. **Bellacosa A, Kumar CC, Di Cristofano A, and Testa JR.** Activation of AKT kinases in cancer: implications for therapeutic targeting. *Adv Cancer Res* 94: 29-86, 2005.

8. **Benigni R and Bossa C.** Alternative strategies for carcinogenicity assessment: an efficient and simplified approach based on in vitro mutagenicity and cell transformation assays. *Mutagenesis* 26: 455-460, 2011.

549 9. **Berking C, Takemoto R, Satyamoorthy K, Shirakawa T, Eskandarpour M,**
550 **Hansson J, VanBelle PA, Elder DE, and Herlyn M.** Induction of melanoma phenotypes in
551 human skin by growth factors and ultraviolet B. *Cancer Res* 64: 807-811, 2004.
552 10. **Cacciotti P, Libener R, Betta P, Martini F, Porta C, Procopio A, Strizzi L, Penengo**
553 **L, Tognon M, Mutti L, and Gaudino G.** SV40 replication in human mesothelial cells
554 induces HGF/Met receptor activation: a model for viral-related carcinogenesis of human
555 malignant mesothelioma. *Proc Natl Acad Sci U S A* 98: 12032-12037, 2001.
556 11. **Cario-Andre M, Bessou S, Gontier E, Maresca V, Picardo M, and Taieb A.** The
557 reconstructed epidermis with melanocytes: a new tool to study pigmentation and
558 photoprotection. *Cell Mol Biol (Noisy-le-grand)* 45: 931-942, 1999.
559 12. **Chang WP and Little JB.** Persistently elevated frequency of spontaneous mutations in
560 progeny of CHO clones surviving X-irradiation: association with delayed reproductive death
561 phenotype. *Mutat Res* 270: 191-199, 1992.
562 13. **DeBerardinis RJ, Mancuso A, Daikhin E, Nissim I, Yudkoff M, Wehrli S, and**
563 **Thompson CB.** Beyond aerobic glycolysis: transformed cells can engage in glutamine
564 metabolism that exceeds the requirement for protein and nucleotide synthesis. *Proc Natl*
565 *Acad Sci U S A* 104: 19345-19350, 2007.
566 14. De Giorgi V, Gori A, Grazzini M, Rossari S, Longo A, Oranges T and Savarese I.
567 Obesity and Melanoma. British J of Dermatol, 1365-2133, 2011.
568 15. **DiPaolo JA, Burkhardt A, Doniger J, Pirisi L, Popescu NC, and Yasumoto S.** In
569 vitro models for studying the molecular biology of carcinogenesis. *Toxicol Pathol* 14: 417-
570 423, 1986.
571 16. **Dubrova YE, Plumb M, Gutierrez B, Boulton E, and Jeffreys AJ.** Transgenerational
572 mutation by radiation. *Nature* 405: 37, 2000.

17. **Eichhoff OM, Zipser MC, Xu M, Weeraratna AT, Mihic D, Dummer R and Hoek KS**. The immunohistochemistry of invasive and proliferative phenotype switching in melanoma: a case report. *Melanoma Res* 20: 349-355, 2010.

18. **Flier JS, Mueckler MM, Usher P, and Lodish HF.** Elevated levels of glucose transport and transporter messenger RNA are induced by ras or src oncogenes. *Science* 235: 1492-1495, 1987.

19. **Guenin S, Schwartz L, Morvan D, Steyaert JM, Poignet A, Madelmont JC, and Demidem A.** PP2A activity is controlled by methylation and regulates oncoprotein expression in melanoma cells: a mechanism which participates in growth inhibition induced by chloroethylnitrosourea treatment. *Int J Oncol* 32: 49-57, 2008.

20. **Hirsch J, Johnson CL, Nelius T, Kennedy R, Riese W, and Filleur S.** PEDF inhibits IL8 production in prostate cancer cells through PEDF receptor/phospholipase A2 and regulation of NFkappaB and PPARgamma. *Cytokine* 55: 202-210, 2011.

21. **Hoek KS and Goding CR.** Cancer stem cells versus phenotype-switching in melanoma *Pigment Cell Melanoma Res* 23:746-59, 2010.

22. **Hursting SD, Nunez NP, Varticovski L, and Vinson C.** The obesity-cancer link: lessons learned from a fatless mouse. *Cancer Res* 67: 2391-2393, 2007.

23. **Janssens V and Goris J.** Protein phosphatase 2A: a highly regulated family of serine/threonine phosphatases implicated in cell growth and signalling. *Biochem J* 353: 417-439, 2001.

24. **Janssens V, Goris J, and Van Hoof C.** PP2A: the expected tumor suppressor. *Curr Opin Genet Dev* 15: 34-41, 2005.

595 25. **Li CY, Little JB, Hu K, Zhang W, Zhang L, Dewhirst MW, and Huang Q.**
596 Persistent genetic instability in cancer cells induced by non-DNA-damaging stress
597 exposures. *Cancer Res* 61: 428-432, 2001.
598 26. **Maddodi N and Setaluri V.** Role of UV in cutaneous melanoma. *Photochem Photobiol*
599 84: 528-536, 2008.
600 27. **McCormick JJ and Maher VM.** Malignant transformation of human skin fibroblasts
601 by two alternative pathways. *Adv Exp Med Biol* 720: 191-207, 2011.
602 28. **Morvan D and Demidem A.** Metabolomics by proton nuclear magnetic resonance
603 spectroscopy of the response to chloroethylnitrosourea reveals drug efficacy and tumor
604 adaptive metabolic pathways. *Cancer Res* 67: 2150-2159, 2007.
605 29. **Morvan D, Demidem A, Guenin S, and Madelmont JC.** Methionine-dependence
606 phenotype of tumors: metabolite profiling in a melanoma model using L-[methyl-
607 13C]methionine and high-resolution magic angle spinning 1H-13C nuclear magnetic
608 resonance spectroscopy. *Magn Reson Med* 55: 984-996, 2006.
609 30. **Nieman KM and Schalinske KL.** Insulin administration abrogates perturbation of
610 methyl group and homocysteine metabolism in streptozotocin-treated type 1 diabetic rats.
611 *Am J Physiol Endocrinol Metab* 301: E560-565, 2011.
612 31. **Palanivel R, Veluthakal R, and Kowluru A.** Regulation by glucose and calcium of the
613 carboxylmethylation of the catalytic subunit of protein phosphatase 2A in insulin-secreting
614 INS-1 cells. *Am J Physiol Endocrinol Metab* 286: E1032-1041, 2004.
615 32. **Pim D, Massimi P, Dilworth SM, and Banks L.** Activation of the protein kinase B
616 pathway by the HPV-16 E7 oncoprotein occurs through a mechanism involving interaction
617 with PP2A. *Oncogene* 24: 7830-7838, 2005.

618 33. **Pleiss C, Risse JH, Biersack HJ, and Bender H.** Role of FDG-PET in the assessment
619 of survival prognosis in melanoma. *Cancer Biother Radiopharm* 22: 740-747, 2007.
620 34. **Rathmell JC, Fox CJ, Plas DR, Hammerman PS, Cinalli RM, and Thompson CB.**
621 Akt-directed glucose metabolism can prevent Bax conformation change and promote growth
622 factor-independent survival. *Mol Cell Biol* 23: 7315-7328, 2003.
623 35. **Sato M, Vaughan MB, Girard L, Peyton M, Lee W, Shames DS, Ramirez RD,**
624 **Sunaga N, Gazdar AF, Shay JW, and Minna JD.** Multiple oncogenic changes (K-
625 RAS(V12), p53 knockdown, mutant EGFRs, p16 bypass, telomerase) are not sufficient to
626 confer a full malignant phenotype on human bronchial epithelial cells. *Cancer Res* 66: 2116-
627 2128, 2006.
628 36. **Sreekumar A, Poisson LM, Rajendiran TM, Khan AP, Cao Q, Yu J, Laxman B,**
629 **Mehra R, Lonigro RJ, Li Y, Nyati MK, Ahsan A, Kalyana-Sundaram S, Han B, Cao X,**
630 **Byun J, Omenn GS, Ghosh D, Pennathur S, Alexander DC, Berger A, Shuster JR, Wei**
631 **JT, Varambally S, Beecher C, and Chinnaiyan AM.** Metabolomic profiles delineate
632 potential role for sarcosine in prostate cancer progression. *Nature* 457: 910-914, 2009.
633 37. **Tokunaga E, Kimura Y, Oki E, Ueda N, Futatsugi M, Mashino K, Yamamoto M,**
634 **Ikebe M, Kakeji Y, Baba H, and Maehara Y.** Akt is frequently activated in HER2/neu-
635 positive breast cancers and associated with poor prognosis among hormone-treated patients.
636 *Int J Cancer* 118: 284-289, 2006.
637 38. **Whiteman DC, Pavan WJ, and Bastian BC.** The melanomas: a synthesis of
638 epidemiological, clinical, histopathological, genetic, and biological aspects, supporting
639 distinct subtypes, causal pathways, and cells of origin. Pigment Cell Melanoma Res 24: 879-
640 897, 2011.
641

642

643 **FIGURE LEGENDS**

644 Figure 1. Chronic insulin and glucose supplementation promotes cell proliferation of human
645 normal melanocytes

646 *(A)* Proliferation curves. Melanocytes were either untreated (UN) or treated with ×2 insulin-
647 glucose (ING and ING*). ING cells are human normal melanocytes (NHM) treated cells 2
648 times a week over the long term. ING* cells are NHM treated for 3 weeks then untreated for
649 4 weeks. At various days, cells were harvested and counted. Data are means of triplicates.
650 Insert, cell count from D0 to D20 in linear scale; bars, ±SD.

651 (*B*) Microscopy examination. Human melanocytes exposed to chronic insulin and glucose
652 supplementation (ING*) exhibit alterations in cell morphology in comparison with untreated
653 melanocytes (UN). Treatment increased cell size with a large cytoplasm and long membrane
654 extensions. Bar, 150 µm.

655 (*C*) Cell cycle analysis. Melanocyte pellets were incubated with 50 µg/µl propidium iodide.
656 The stained cells were run in an EPICS XL flow cytometer, and data was analyzed with
657 MultiCycle software. The proportion of cells in the G1, G2 and S phase of the cell cycle is
658 displayed for 3 conditions (UN, ING, and ING*). Bars, SD.

659

660 Figure 2. Chronic insulin and glucose supplementation promotes soft agar colony formation

661 (*A*) Pictures of colonies on soft agar. Cells were included in soft agar as described in the
662 Materials and Methods section and incubated at 37°C. Plates were stained with 0.005%
663 crystal violet for 1 h. ING and ING* cells were grown in agar, after culture as monolayer in
664 their specific medium for 3 weeks. ING cells were continuously treated while ING* were

665 untreated in agar. For comparison, B16 melanoma and L929 fibroblast cells that are able to
666 form colony is also shown.
667 (*B*) Colony number. Colonies were counted by use of a dissecting microscope. The count of
668 colonies was performed for 15 days for untreated (UN) normal human melanocytes (NHM),
669 ING and ING* cells, derived from NHM, L929 cells and B16 melanoma tumor cells. Data
670 are the mean number of colonies formed in three plates, for each group. Bars, ±SD.
671
672 Figure 3. Chronic insulin and glucose supplementation provokes DNA and chromosomal
673 alterations
674 (*A*) DNA content in ING and ING* cells. At day 35 and day 45, cells from each group were
675 harvested and DNA was extracted as described in the Materials and Methods section. Bars,
676 SD; *$P < 0.05$, ING or ING* *vs* UN.
677 (*B*) Untreated human normal melanocytes (UN) and glucose-insulin treated cells derived
678 from human normal melanocytes (ING*) were cultured as monolayer in culture flasks until
679 70% confluence and then treated with colchicine at (0.01 µg/ml) during 17 to 57 h. ING*
680 cells have an increased amount of chromosomes and their chromosome arms are extended
681 (arrows) which may indicate activation of telomerases.
682
683 Figure 4. Chronic insulin and glucose supplementation upregulates oncoproteins and
684 decreases PP2A activity.
685 *(A*) Oncoprotein and PP2A protein expression. Western Blot of PP2AC, PP2AC-Met+, Akt,
686 P-Akt, c-Myc, PTEN, P-PTEN, PP1, Ras and β-tubulin proteins were performed in untreated
687 human melanocytes (UN), ×2 insulin and glucose-supplemented cells (ING and ING*). ING

cells correspond to human melanocytes treated by insulin-glucose over the long term. ING* corresponds to human melanocytes treated by insulin-glucose for 3 weeks then replaced in standard medium.

(*B*) Densitometric quantification of PP2A and oncoprotein expression. Measurements were obtained in ING, ING* and IPC cells, relative to expression in untreated normal human melanocytes (UN). Quantification is done by normalization to tubulin expression. Data are means of at least 3 independent experiments. ND, not done; bars, SD; *, P<0.05 (ING and ING* pooled together vs UN).

(*C)* Effect of an antagonist of PP2A methylation, okadaic acid (OA), on untreated human normal melanocytes (UN). Western Blot analysis after OA treatment at 5 nM for 48 h of methylated PP2AC (PP2AC-Met+), P-Akt, c-Myc, and β-tubulin.

(*D)* PP2A activity. The human melanoma cell line IPC 227 was used as a comparison. PP2A activity was determined as described in Materials and Methods. It was measured in ING, ING* and IPC cells relative to that in untreated normal human melanocytes (UN). Data are means of two independent experiments; bars, *S.D*. *$P<$ 0.05, ING or ING* *vs* UN, **$P<$ 0.01, IPC *vs* UN.

Figure 5. Chronic insulin and glucose supplementation induces glycolysis changes

(*A*) Bioenergetics-related transcriptomics data (n=20). Transcripts are classified in decreasing order of variation in ING* cells relative to UN cells. Genes varying significantly include *Hif1a*, *Pgk1*, *Acly* and *Pfkfb3*. See Table 2 for gene description. Bars, SD; *, P<0.05; **, P<0.01.

(*B*) Pyruvate kinase-M2 activity. Cells were harvested and proteins were extracted. The activity of PK-M2 enzyme was determined as described in the Materials and Methods

712 section. For comparison, PK-M2 activity of a human ocular melanoma cell line, IPC 227, is
713 shown. Bars, SD; **, *P*<0.01, ING, ING* or IPC *vs* UN cells.
714
715 Figure 6. Chronic insulin and glucose supplementation induces cellular redistribution of
716 methyl group metabolism
717 (*A*) Proton NMR spectra of UN, ING* and IPC cells. UN, untreated human normal
718 melanocytes (NHM); ING*, melanocytes exposed to chronic insulin-glucose
719 supplementation, derived from NHM, and IPC 227 F, human ocular melanoma cell line.
720 Abbreviations: Cr, creatine; GA, guanidinoacetate; Gly, glycine; GPC,
721 glycerophosphocholine; PC, phosphocholine; Sar, sarcosine; GSH, glutathione; OAA,
722 oxaloacetate; Pyr, pyruvate; Glu, glutamate; Ala, alanine; FA, fatty acids.
723 (*B*) Cytoplasmic or nuclear protein methylation. Methyl group incorporation was
724 determined as described in Materials and Methods. Data are means of 3 independent
725 experiments. Bars, SD; *, *P*<0.05, ING* *vs* UN; **, *P*<0.01, ING* *vs* UN.
726 (*C*) Effect of insulin and glucose supplementation on DNA methylation. Data are means of 3
727 independent experiments. Bars, SD; *, *P*<0.05, ING or ING* *vs* UN.
728
729 Figure 7. Scheme showing the actors of PP2A carboxymethylation and PP2A regulation of
730 oncoproteins
731 A, B, C, subunits of PP2A protein. PP2A methylation results from the opposing effects of
732 specific leucine methyltransferase (LCMT-1) or protein phosphatase methylesterase (PME-
733 1). LCMT-1 uses S-adenosylmethionine (SAM) as a substrate. In this study, insulin-glucose
734 supplementation decreases carboxymethylation of PP2A. Targeting may result from
735 inhibition of LCMT1, activation of PME-1, and/or rerouting of SAM metabolism.

736

737

738 **TABLE LEGENDS**

739 Table 1. Doubling time of cell proliferation. Human normal melanocytes were exposed to
740 different concentrations of glucose and insulin from ×1 to ×50 the standard medium
741 concentration. Data are means of 3 independent experiments.

742

743 Table 2. Transcriptomics data of ING* melanocytes. Transcripts (n=89) are classified in 6
744 clusters. Gene acronym is given, together with the corresponding protein name, the variation
745 of expression in ING* cells relative to that in UN cells, the ratio of expression in ING* cells
746 relative to that in UN cells and the *P* value of the t-test. Data are means of 3 independent
747 experiments.

748

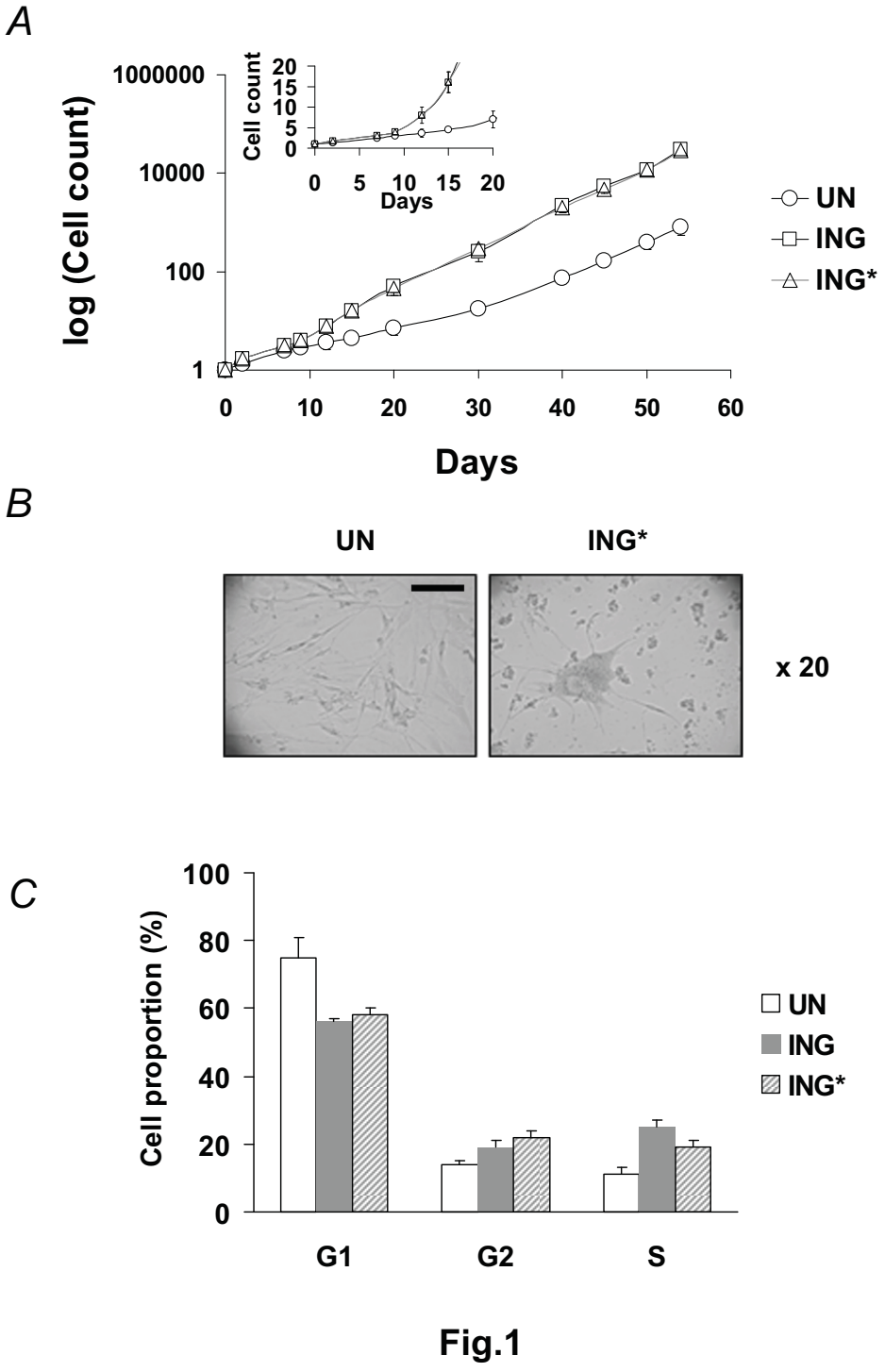
A
log (Cell count)
1000000
10000
100
1
0
10
20
30
40
50
60
Days
Cell count
20
15
10
5
0
0
5
10
15
20
Days
UN
ING
ING*
B
UN
ING*
x 20
C
Cell proportion (%)
100
80
60
40
20
0
G1
G2
S
UN
ING
ING*

Fig.1

A

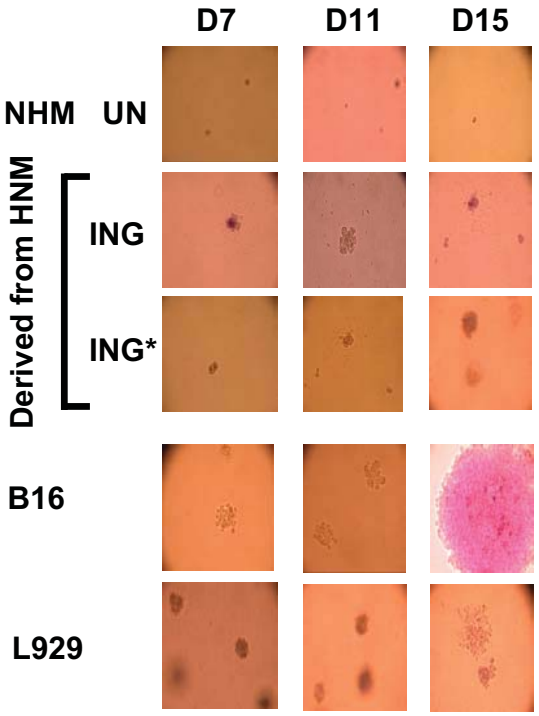
D7
D11
D15
NHM
UN
Derived from HNM
ING
ING*
B16
L929

B

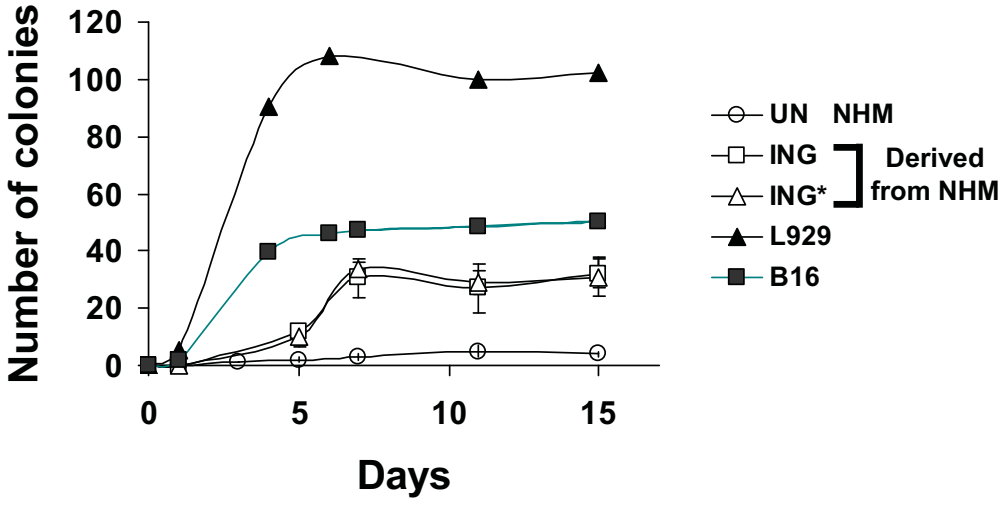
Number of colonies
120
100
80
60
40
20
0
0
5
10
15
Days
UN
NHM
ING
ING*
Derived from NHM
L929
B16

Fig. 2

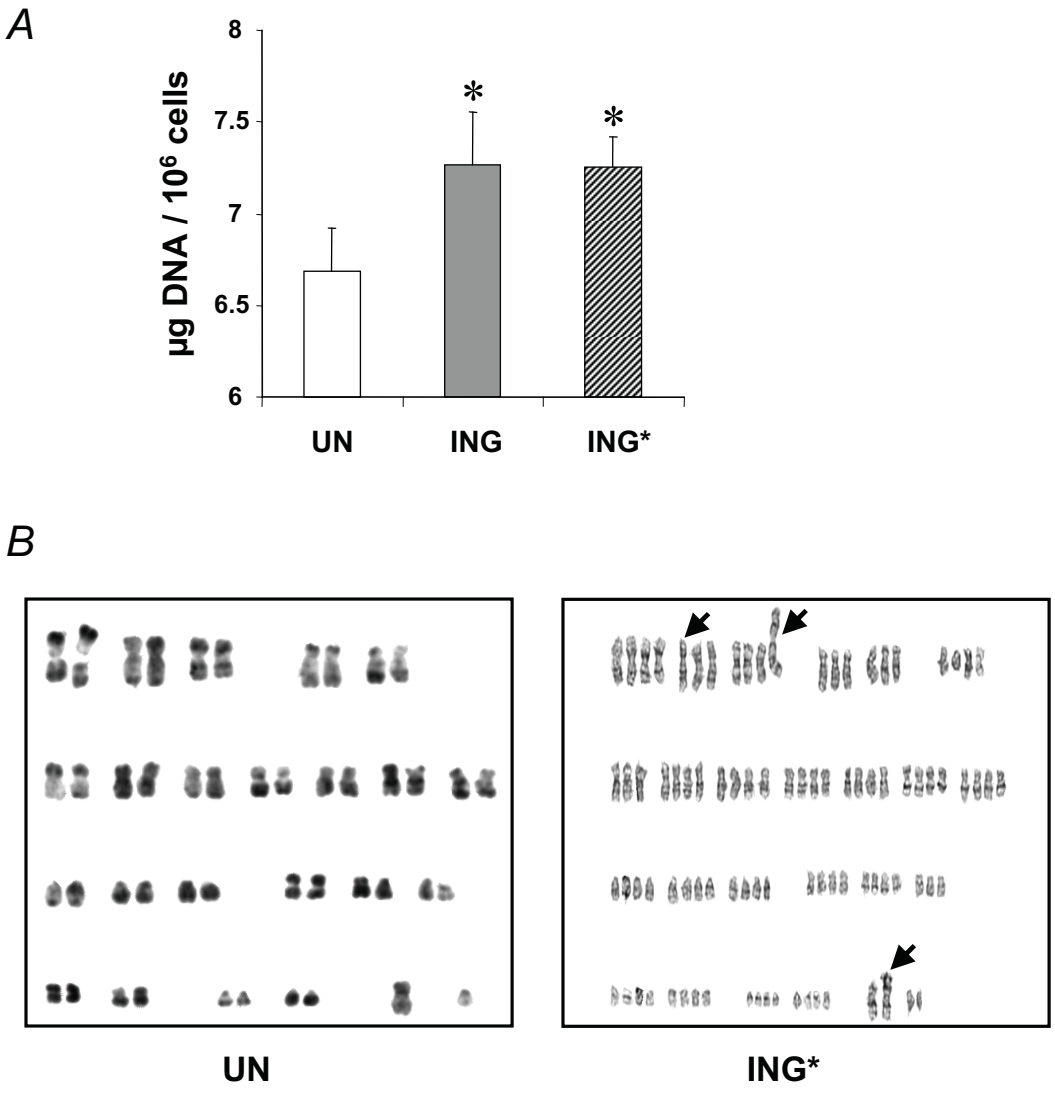

Fig. 3

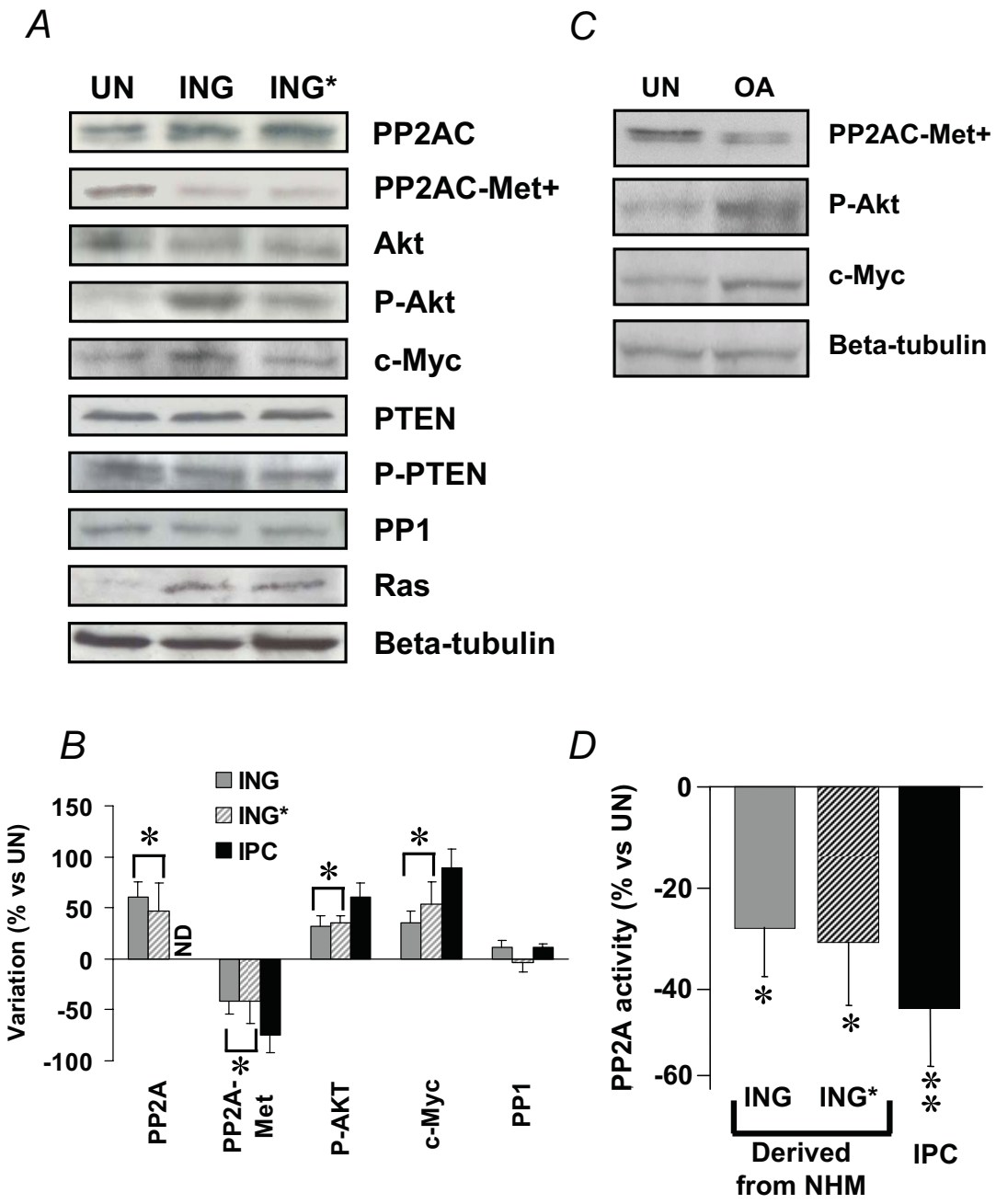
A
UN
ING
ING*
PP2AC
PP2AC-Met+
Akt
P-Akt
c-Myc
PTEN
P-PTEN
PP1
Ras
Beta-tubulin
C
UN
OA
PP2AC-Met+
P-Akt
c-Myc
Beta-tubulin
B
ING
ING*
IPC
Variation (% vs UN)
150
100
50
0
-50
-100
ND
PP2A
PP2A-Met
P-AKT
c-Myc
PP1
D
PP2A activity (% vs UN)
0
-20
-40
-60
ING
ING*
Derived from NHM
IPC

Fig. 4

A

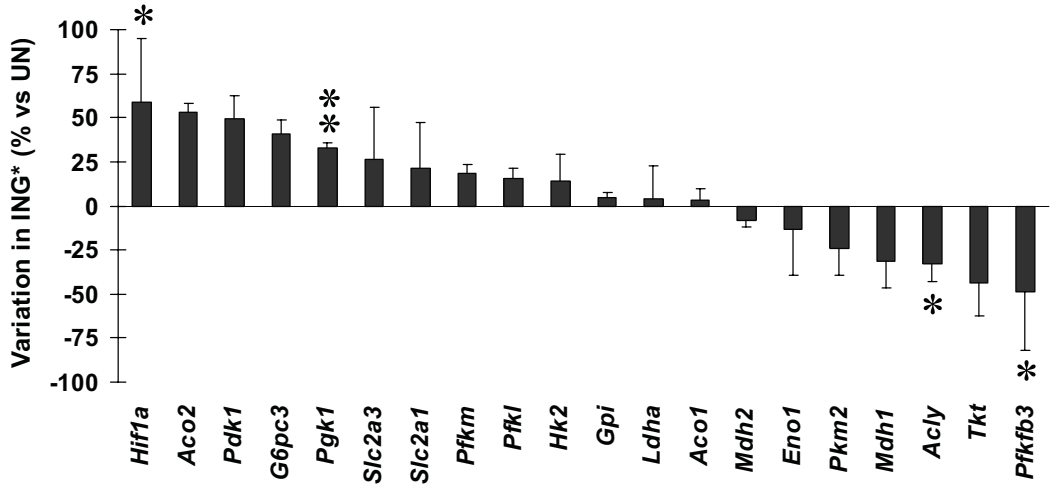
Variation in ING* (% vs UN)
100
75
50
25
0
-25
-50
-75
-100
*
**
*
*
Hif1a
Aco2
Pdk1
G6pc3
Pgk1
Slc2a3
Slc2a1
Pfkm
Pfkl
Hk2
Gpi
Ldha
Aco1
Mdh2
Eno1
Pkm2
Mdh1
Acly
Tkt
Pfkfb3

B

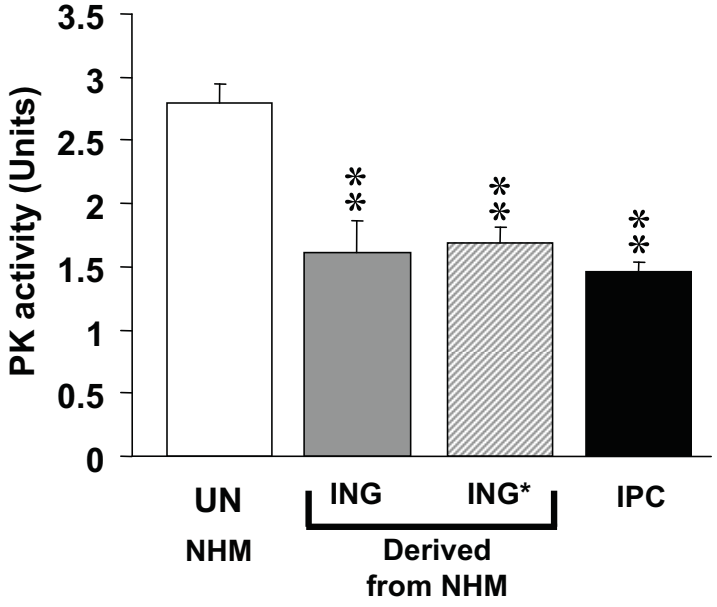
PK activity (Units)
3.5
3
2.5
2
1.5
1
0.5
0
**
**
**
UN
NHM
ING
ING*
Derived
from NHM
IPC

Fig. 5

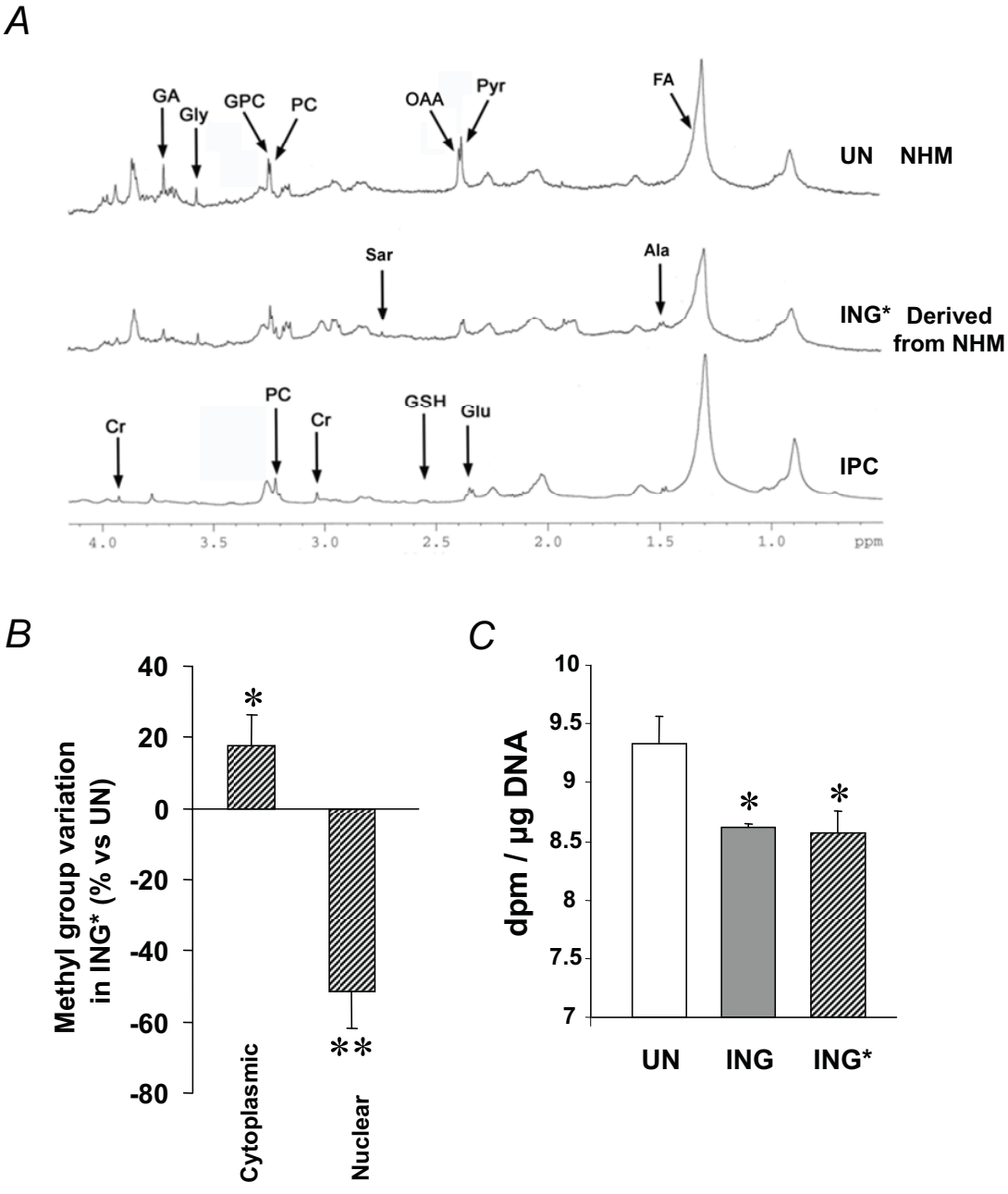
A
GA
Gly
GPC
PC
OAA
Pyr
FA
UN NHM
Sar
Ala
ING* Derived from NHM
Cr
PC
Cr
GSH
Glu
IPC
4.0
3.5
3.0
2.5
2.0
1.5
1.0
ppm
B
Methyl group variation in ING* (% vs UN)
40
20
0
-20
-40
-60
-80
Cytoplasmic
Nuclear
C
dpm / µg DNA
10
9.5
9
8.5
8
7.5
7
UN
ING
ING*

Fig. 6

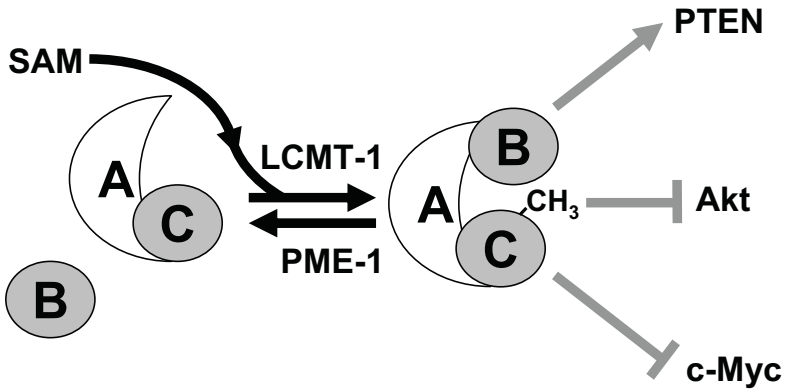

Fig. 7

Insulin and Glucose concentration (x Standard medium concentration)	Doubling time (Days)
1	5.2
2	2.7
5	3.4
7	3.5
10	3.4
50	15

Table 1.
Doubling time of melanocytes according to insulin-glucose concentration

Gene	Protein	Variation (%)	Ratio (-)	*P* value
Cell cycle and Signalling				
Ccnd1	cyclin D1	52.14	1.52	0.037
Cdkn2a	cyclin-dependent kinase inhibitor 2A (melanoma, p16, inhibits CDK4)	126.12	2.26	0.015
Cdkn1a	cyclin-dependent kinase inhibitor 1A (p21, Cip1)	-23.61	0.76	0.113
Cdkn1b	cyclin-dependent kinase inhibitor 1B (p27, Kip1)	-0.43	1.00	0.453
Casp3	caspase 3, apoptosis-related cysteine peptidase	-6.13	0.94	0.327
Il8	interleukin 8	98.97	1.99	0.007
Insr	insulin receptor	9.71	1.10	0.017
Mitf	microphthalmia-associated transcription factor	22.90	1.23	0.184
Aqp1	aquaporin 1 (Colton blood group)	46.88	1.47	0.274
Nfkb2	nuclear factor of κ light polypeptide gene enhancer in B-cells 2	-6.73	0.93	0.165
Nfkb1	nuclear factor of κ light polypeptide gene enhancer in B-cells 1	0.65	1.01	0.477
Stk11	serine/threonine kinase 11	13.71	1.14	0.116
Oncoproteins and PP2A				
Pten	phosphatase and tensin homolog	-24.64	0.75	0.100
Myc	v-myc myelocytomatosis viral oncogene homolog	-29.08	0.71	0.071
Hras	v-Ha-ras Harvey rat sarcoma viral oncogene homolog	-6.71	0.93	0.155
Jun	jun oncogene	5.87	1.06	0.329
Junb	jun B proto-oncogene	-16.72	0.83	0.091
Braf	v-raf murine sarcoma viral oncogene homolog B1	-19.05	0.81	0.351
Kras	v-Ki-ras2 Kirsten rat sarcoma viral oncogene homolog	-18.98	0.81	0.069
Akt1	v-akt murine thymoma viral oncogene homolog 1	6.20	1.06	0.241
Jund	jun D proto-oncogene	-8.00	0.92	0.338
Fos	v-fos FBJ murine osteosarcoma viral oncogene homolog	-32.47	0.68	0.107
Nras	neuroblastoma RAS viral (v-ras) oncogene homolog	-37.77	0.62	0.044
Bax	BCL2-associated X protein	9.45	1.09	0.172
Bcl2	B-cell CLL/lymphoma 2	-1.28	0.99	0.480
Rela	v-rel reticuloendotheliosis viral oncogene homolog A	21.08	1.21	0.095
Pink1	PTEN induced putative kinase 1	71.23	1.71	0.038
Tp53	tumor protein p53	-8.12	0.92	0.241
Mdm2	Mdm2 p53 binding protein homolog (mouse)	6.22	1.06	0.457
Rb1	retinoblastoma 1	-22.38	0.78	0.028

Relb	v-rel reticuloendotheliosis viral oncogene homolog B	-27.70	0.72	0.077
Kit	v-kit Hardy-Zuckerman 4 feline sarcoma viral oncogene homolog	-42.07	0.58	0.133
Ppp2cb	protein phosphatase 2 (formerly 2A), catalytic subunit, β isoform	-7.76	0.92	0.273
Ppp2ca	protein phosphatase 2 (formerly 2A), catalytic subunit, α isoform	-8.85	0.91	0.173
Ppp2r5c	protein phosphatase 2, regulatory subunit B', γ isoform	45.23	1.45	0.365
Ppp2r1a	protein phosphatase 2 (formerly 2A), subunit A, α isoform	43.73	1.44	0.023
Ppp2r1b	protein phosphatase 2 (formerly 2A), subunit A, β isoform	-3.77	0.96	0.110
Ptpra	protein tyrosine phosphatase, receptor type, A	7.51	1.08	0.265
Prkaa1	protein kinase, AMP-activated, α 1 catalytic subunit	1.03	1.01	0.474
Ppme1	protein phosphatase methylesterase 1	-6.56	0.93	0.390
Ppp1ca	protein phosphatase 1, catalytic subunit, α isoform	-37.80	0.62	0.037
Ppp1cb	protein phosphatase 1, catalytic subunit, β isoform	8.43	1.08	0.235
Bioenergetic Metabolism				
Slc2a1	solute carrier family 2 (glucose transporter), member1	21.40	1.21	0.102
Slc2a3	solute carrier family 2 (glucose transporter), member 3	26.25	1.26	0.075
Hk2	hexokinase 2	13.97	1.14	0.461
G6pc3	glucose 6 phosphatase, catalytic, 3	41.03	1.41	0.060
Gpi	glucose phosphate isomerase	4.52	1.05	0.187
Pfkl	phosphofructokinase, liver	15.65	1.16	0.061
Pfkm	phosphofructokinase, muscle	18.20	1.18	0.128
Pfkfb3	6-phosphofructo-2-kinase/fructose-2,6-biphosphatase 3	-48.52	0.51	0.033
Tkt	transketolase	-43.53	0.56	0.081
Pgk1	phosphoglycerate kinase 1	33.03	1.33	0.007
Eno1	enolase 1, (alpha)	-13.60	0.86	0.228
Pkm2	pyruvate kinase, muscle	-23.99	0.76	0.083
Ldha	lactate dehydrogenase A	4.01	1.04	0.383
Pdk1	pyruvate dehydrogenase kinase, isozyme 1	49.25	1.49	0.077
Mdh2	malate dehydrogenase 2, NAD (mitochondrial)	-8.08	0.92	0.104
Mdh1	malate dehydrogenase 1, NAD (soluble)	-31.46	0.69	0.170
Aco1	aconitase 1, soluble	3.39	1.03	0.154
Aco2	aconitase 2, mitochondrial	53.30	1.53	0.056
Hif1a	hypoxia inducible factor 1, alpha subunit	58.88	1.59	0.041
Lipid Metabolism				

Acly	ATP citrate lyase	-32.96	0.67	0.023
Acaca	acetyl-Coenzyme A carboxylase alpha	-28.15	0.72	0.137
Fasn	fatty acid synthase	-69.66	0.30	0.050
Pla2g12a	phospholipase A2, group XIIA	39.82	1.40	0.217
Pla2r1	phospholipase A2 receptor 1, 180kDa	102.73	2.03	0.022
Plcb4	phospholipase C, beta 4	23.59	1.24	0.042
Plcb3	phospholipase C, beta 3 (phosphatidylinositol-specific)	-26.63	0.73	0.995
Plcb2	phospholipase C, beta 2	-67.58	0.32	0.108
Pld1	phospholipase D1, phosphatidylcholine-specific	45.43	1.45	0.088
Chka	choline kinase alpha	-1.46	0.99	0.417
Pcyt1a	phosphate cytidylyltransferase 1, choline, alpha	6.81	1.07	0.273
Pcyt1b	phosphate cytidylyltransferase 1, choline, beta	140.46	2.40	0.025
Chpt1	choline phosphotransferase 1	30.68	1.31	0.032
Chkb;Cpt1b	choline kinase-like, carnitine palmitoyltransferase 1B	66.37	1.66	0.071
Etnk1	ethanolamine kinase 1	29.53	1.30	0.066
Methyl Group Metabolism				
Pemt	phosphatidylethanolamine N-methyltransferase	31.41	1.31	0.080
Lcmt1	leucine carboxyl methyltransferase 1	25.78	1.26	0.018
Mgmt	O-6-methylguanine-DNA methyltransferase	32.29	1.32	0.004
Other Metabolic Pathways and Oxidative Stress				
Mlxipl	MLX interacting protein-like	-100.00		0.078
Txnrd1	thioredoxin reductase 1	71.70	1.72	0.034
Cat	catalase	22.16	1.22	0.071
Gpx1	glutathione peroxidase 1	14.71	1.15	0.279
Gsr	glutathione reductase	-9.16	0.91	0.007
Gss	glutathione synthetase	18.82	1.19	0.045
Gls	glutaminase	15.86	1.16	0.198
Glul	glutamate-ammonia ligase (glutamine synthetase)	-30.59	0.69	0.157
Got1	glutamic-oxaloacetic transaminase 1, soluble	-4.68	0.95	0.413
Tyr	tyrosinase (oculocutaneous albinism IA)	-54.89	0.45	0.013

Table 2

Transcriptomic data of ING melanocytes in comparison to untreated melanocytes.*